Measurement of the electron affinity of the lanthanum atom

Yuzhu Lu,[1] Rulin Tang,[1] Xiaoxi Fu,[1] and Chuangang Ning[1,2,*]

[1]*Department of Physics, State Key Laboratory of Low Dimensional Quantum Physics, Tsinghua University, Beijing 10084, China*
[2]*Collaborative Innovation Center of Quantum Matter, Beijing, China*

Atomic lanthanum anion La$^-$ is the best candidate for laser cooling of any atomic anions found so far. The bound-bound electric dipole transitions of La$^-$ have been identified and measured. Theoretical studies have shown that La$^-$ has a very complicated electronic structure, which cannot be well resolved by the traditional photoelectron spectroscopy. In the present work, we report high-resolution photoelectron spectroscopy of La$^-$ via the slow-electron velocity-map imaging method in combination with an ion trap. The electron affinity of La was determined to be 4496.97(20) cm^{-1} or 0.557 553(25) eV. In addition, the energy levels of La$^-$, $^3F_3^e$, $^3F_4^e$, $^1D_2^e$, $^1D_2^o$, $^3P_0^e$, $^3P_1^e$, and $^3P_2^e$, were also determined.

I. INTRODUCTION

Negative ions usually have very few bound states in contrast with their neutral and positive counterparts due to the weak binding of an extra electron. Only a few atomic anions have bound excited states of opposite parity to their ground states, which is required for the electric dipole transition used for laser cooling. Laser cooling of anions was proposed by Kellerbauer and Walz to sympathetically cool antiprotons and then enhance the production of antihydrogen [1]. Moreover, it is possible to produce ultracold negative ions by sympathetic cooling with the help of laser-cooled anions, opening up a brand new field of ultracold physics [2].

So far, only Os$^-$ [3–6], La$^-$ [7,8], and Ce$^-$ [9,10] are confirmed to have opposite parity bound states by experiments. The previous experimental and theoretical studies have shown that La$^-$ is the most promising candidate for laser cooling of any atomic anions. Several electric dipole transitions of La$^-$ have been identified via tunable infrared spectroscopy [8,11], and the resonant frequency of the laser-cooling transition $^3F_2^e \rightarrow {}^3D_1^o$ has been determined to be 96.592 713(91) THz [12]. However, the electron affinity (EA) of La still remains poorly measured. EA is a fundamental parameter that measures the capability of an atom to form the corresponding negative ion. The measurement of EA is essential for understanding the electron-electron correlation in negative ions.

The photoelectron energy spectrum of La$^-$ is very complicated due to the partially filled 5d subshell. In 1998, Covington *et al.* measured the EA value of La via the traditional laser photoelectron energy spectroscopy (LPES) method [13]. Their experiment indicated that the EA of La should be 0.47 ± 0.02 eV and there should be at least one exited state bounded by 0.17 ± 0.02 eV. However, most of the fine structures were not resolved in their spectrum due to the limited energy resolution. In 2009, O'Malley and

Beck [14] carried out relativistic configuration interaction (RCI) calculations in which seven even states (5$d^2$6s^2) and eight odd states (5d6$s^2$6p) were predicted. They also showed that the ground state configuration of La$^-$ was 5$d^2$6s^2 instead of 5d6$s^2$6p as previously believed [15–17] and the EA value was calculated to be 0.545 eV.

Later, the LPES experiment by Covington *et al.* was reinterpreted by Pan and Beck via RCI calculations in 2016 [18]. The EA of La was revised to be 0.550 eV. Binding energies of other states were also revised. The calculated energy levels agree well with the previous experimental results.

Once the EA of La is determined, all binding energies of the odd states except $^3P_0^o$, as well as the even states $^3F_3^e$ and $^3F_4^e$ recognized by O'Malley and Beck's calculations [18], can be obtained based on the experiment of Walter *et al.* [8]. In the present work, we utilize the slow-electron velocity-map imaging (SEVI) method [19–21] in combination with an ion trap to measure the EA value of La. SEVI has a very high-energy resolution, typically a few cm^{-1} near the photodetachment threshold. This is an essential ability for resolving the dense electronic states of La$^-$. With SEVI, we have successfully determined the EA values of several transitional elements with uncertainties typically less than 1 cm^{-1} [22–25]. Recently, a cryogenically controlled ion trap [26,27] was installed on our apparatus. As demonstrated in our recent works for measuring the EAs of titanium [28] and hafnium [29], the cryogenic ion trap can effectively enhance the intensity of negative ions. This is an important feature for acquiring a strong enough negative ion beam for elements with very low EA values. In addition, an ion trap is helpful for identifying the excited states with ∼10-ms lifetimes since their intensities will change during the trapping period. The excited states with long lifetimes usually have no allowed electric dipole transitions to the ground state. Therefore, they cannot be directly observed via the infrared resonant spectroscopy. The states observed in the present work are complementary to the previous investigations. Moreover, the cryogenic ion trap can effectively cool molecular anions down to a temperature as low as ∼10 K, which can substantially improve the sharpness and cleanness

---

*ningcg@tsinghua.edu.cn
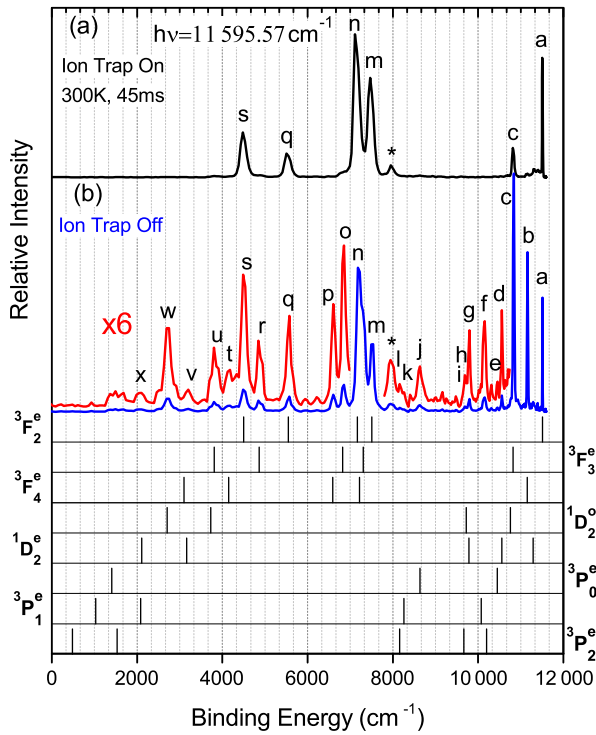
FIG. 1. Photoelectron spectra of La$^-$ at photon energy $h\nu = 11\,595.57\,\text{cm}^{-1}$ obtained with the trap-on mode (a) and the trap-off mode (b). In the trap-on mode, the ions are trapped for 45 ms, and are then thrown out for further analyzing. In the trap-off mode, the ions directly fly through the ion trap as the trap is turned off. The red curve shows the weak peaks multiplied by a factor of 6 for a clearer view. The sticks below the spectra indicate the binding energy of photodetachment channels from the states labeled on the left or right sides. The related transitions are illustrated in Fig. 2.

of the photoelectron energy spectra of polyatomic molecular anions [28,29]. The precooled La$^-$ with a temperature $\sim$10 K can also significantly reduce the cooling time to reach Doppler temperature [12].

II. EXPERIMENT SETUP

Our SEVI apparatus has been described in detail previously [28,30]. Briefly, the apparatus consists of a laser ablation ion source, a cold ion trap, a Wiley-McLaren type time of-flight (TOF) mass spectrometer [31], and a photoelectron velocity-map imaging (VMI) system [32]. The La$^-$ ions are produced by focusing the second-harmonic output of a Nd: YAG laser (532 nm, 20 Hz, $\sim$10 mJ/pulse) on a rotating and translating lanthanum metal disk. The negative ions are accumulated and trapped in an octupole radio-frequency ion trap for 45 ms. The ion trap is mounted on the second stage of a liquid helium refrigerator with a variable temperature 5–300 K. The trapped ions lose their energy through collisions with the buffer gas (a mixture of H$_2$ and He with a ratio 20:80). The ion trap can be turned off, so that ions can directly fly through it. The extracted ions are accelerated by a -1000-V high-voltage pulse in the TOF mass spectrometer. The ions of interest are selected by a mass gate and then photodetached by a tunable dye laser (400–920 nm, linewidth 0.06 cm^{-1} at 625 nm) pumped by a Quanta-Ray Pro 290 Nd:YAG laser (20 Hz, 1000 mJ/pulse at 1064 nm). The photoelectrons are projected onto a phosphor screen behind a set of microchannel plates and recorded by a charge-coupled device (CCD) camera. A real-time intensity weighted centroid program is applied to reconstruct the position of each photoelectron. Typically, 30 000–50 000 laser shots are assembled to form one photoelectron image. The photon energy ($h\nu$) is further measured by a HighFinesse WS6-600 wavelength meter with an
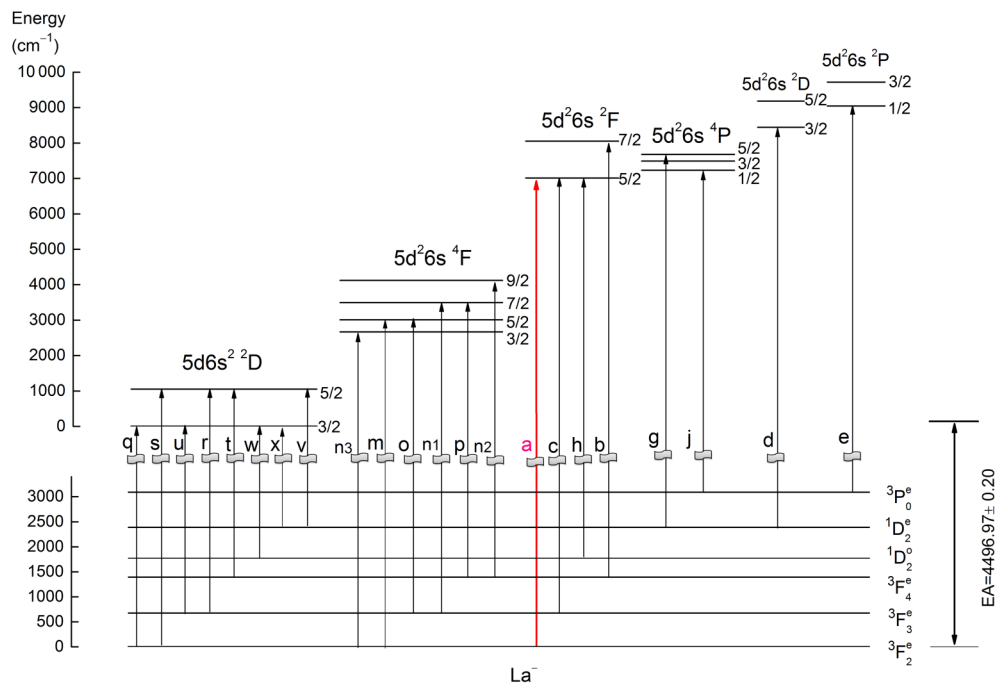
FIG. 2. Partial energy levels of La and La$^-$. The transitions' labels are corresponding to the peaks observed in Fig. 1. Transition a is used to measure the EA value of La.
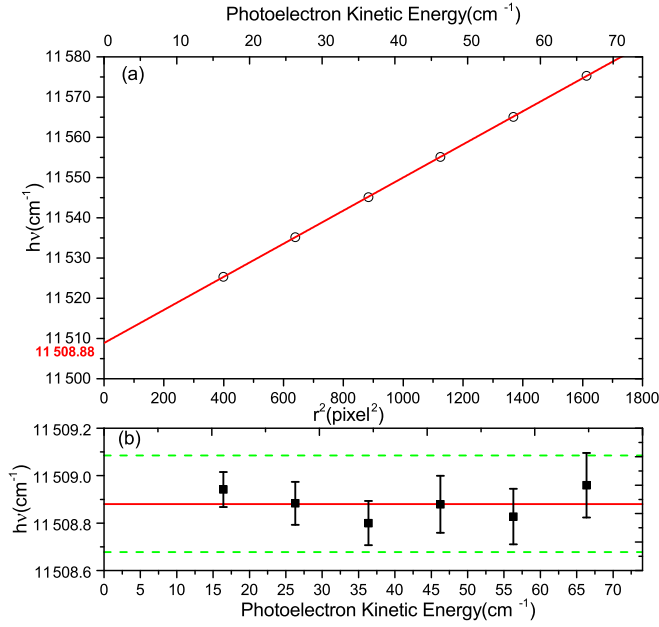
FIG. 3. The photon energy $h\nu$ versus the squared radius r^2 of the measured electron spherical shell for transition a. The solid line is the linear least squares fitting. The intercept $11\,508.88\,\text{cm}^{-1}$ is the binding energy of photodetachment channel a (a). The binding energy of transition $\text{La}(^2F^e_{5/2}) \leftarrow \text{La}^-(^3F^e_2)$ as a function of the kinetic energy of photoelectrons. The dashed lines indicate the uncertainty of $\pm 0.20\,\text{cm}^{-1}$ (b). The uncertainty includes the statistical and fitting error. The systematic error is estimated to be $0.1\,\text{cm}^{-1}$

accuracy of $0.02\,\text{cm}^{-1}$. The maximum entropy velocity Legendre reconstruction (MEVELER) method is used to reconstruct the photoelectron spectrum from the raw image [33].

III. RESULTS AND DISCUSSION

Figure 1 shows the photoelectron energy spectra of La^- at the photon energy $h\nu = 11\,959.57\,\text{cm}^{-1}$. The imaging voltage is -650 V. In Fig. 1(a), La^- ions were stored in the trap for 45 ms at room temperature, so only states with lifetimes comparable with 45 ms can appear in the spectrum. In Fig. 1(b), more peaks were observed when the ion trap was turned off. The extra peaks are related to the short-lived excited states. In the trap-off mode, it takes about 0.4 ms for the La^- ions to fly from the ion source to the photodetachment zone. Therefore, the short-lived excited states have more chance to survive compared with the trap-on mode. It should be pointed out that the higher state $^3D^o_1$ of the potential laser-cooling transition cannot be observed in the present experiment due to its relatively short lifetime $22.1\,\mu s$ [12]. According to the trends of peak intensity, the energy levels of neutral La [34], and the well-known energy gaps of La^- determined by the infrared resonant spectroscopy, as well as the calculations by Pan and Beck [18], most of the peaks observed in Fig. 1 can be identified except the weak peak labeled with an asterisk (*). This peak is not likely from a molecular contaminant with the same mass as the La atom because there is no thermal broadening in the spectra. The generated ions from our laser ablation ion source are usually very hot. The typical temperature

TABLE I. Photodetachment transitions observed in the present work.

Peak	Transition $\text{La}^- \rightarrow \text{La}$	Measured binding energy (cm^{-1})	Assigned binding energy $(\text{cm}^{-1})^a$
a	$^3F^e_2 \rightarrow {}^2F^e_{5/2}$	11508.88(20)	11508.88(20)
b	$^3F^e_4 \rightarrow {}^2F^e_{7/2}$	11154.68(25)	11154.68(35)
c	$^3F^e_3 \rightarrow {}^2F^e_{5/2}$	10831.82(29)	10831.82(38)
d	$^1D^e_2 \rightarrow {}^2D^e_{3/2}$	10553.68(30)	10553.68(30)
e	$^3P^e_0 \rightarrow {}^2P^e_{1/2}$	10449.5 (30)	10449.5(30)
f_1	$^3P^e_2 \rightarrow {}^2P^e_{3/2}$	10171(60)	10171(60)
f_2	$^3P^e_1 \rightarrow {}^2P^e_{1/2}$	10111(60)	10111(60)
g	$^1D^e_2 \rightarrow {}^4P^e_{5/2}$	9788.9(27)	9787.57(30)
h	$^1D^o_2 \rightarrow {}^2F^e_{5/2}$	9712 (60)	9718.71(24)
i	$^3P^e_2 \rightarrow {}^2D^e_{5/2}$	9678(60)	9636(60)
j	$^3P^e_0 \rightarrow {}^4P^e_{1/2}$	8636.7(50)	8636.7(30)
k	$^3P^e_1 \rightarrow {}^4P^e_{1/2}$	8261(60)	8298(60)
l	$^3P^e_2 \rightarrow {}^4P^e_{5/2}$	8161(60)	8132(60)
m	$^3F^e_2 \rightarrow {}^4F^e_{5/2}$	7505.1 (61)	7506.97(20)
n_1	$^3F^e_3 \rightarrow {}^4F^e_{7/2}$	7321(16)	7314.44(38)
n_2	$^3F^e_4 \rightarrow {}^4F^e_{9/2}$	7240(33)	7224.09(35)
n_3	$^3F^e_2 \rightarrow {}^4F^e_{3/2}$	7180(16)	7165.16(20)
o	$^3F^e_3 \rightarrow {}^4F^e_{5/2}$	6825.9(61)	6829.91(38)
p	$^3F^e_4 \rightarrow {}^4F^e_{7/2}$	6590(11)	6597.05(35)
q	$^3F^e_2 \rightarrow {}^2\tilde{D}^e_{5/2}$	5549.3(83)	5550.13(20)
r	$^3F^e_3 \rightarrow {}^2\tilde{D}^e_{5/2}$	4870(13)	4873.07(38)
s	$^3F^e_2 \rightarrow {}^2\tilde{D}^e_{3/2}$	4498(10)	4496.97(20)
t	$^3F^e_4 \rightarrow {}^2\tilde{D}^e_{5/2}$	4156(35)	4155.68(35)
u	$^3F^e_3 \rightarrow {}^2\tilde{D}^e_{3/2}$	3820(35)	3819.91(38)
v	$^1D^e_2 \rightarrow {}^2\tilde{D}^e_{5/2}$	3192(37)	3160.79(30)
w^b	$^1D^o_2 \rightarrow {}^2\tilde{D}^e_{3/2}$	2726(40)	2706.80(24)
	$^3F^o_2 \rightarrow {}^2\tilde{D}^e_{5/2}$		2778.09(31)
x	$^1D^e_2 \rightarrow {}^2\tilde{D}^e_{3/2}$	2087(45)	2107.63(30)

^{a}Deduced value according to the assignment, the measured EA value, the optimized binding energy of transitions measured in the present work, the relative energy gaps measured by Walter *et al.* [8], and the energy levels of neutral La [34].
^{b}Peak w may include the contribution from transition $^3F^o_2 \rightarrow {}^2\tilde{D}^e_{5/2}$ as suggested by the theoretical calculations [18,37].

of ions is ~800 K [30]. It should be noted that the binding energy of peak "*" is $7995.4(58)\,\text{cm}^{-1}$, which matches that of the transition $\text{La}\,(5d^26s\,{}^4F^e_{7/2}) \leftarrow \text{La}^-\,(5d^26s^2\,{}^3F^e_2)$ $(7991.50\,\text{cm}^{-1})$. However, this transition is forbidden by the selection rule within LS coupling [35] and is not predicted by Pan and Beck [18]. Peaks a, m, n_3, q, and s are contributed by the photodetachment from the ground state of La^- $(^3F^e_2)$. In the present work, the strong peak a, which corresponds to the transition $\text{La}(^2F^e_{5/2}) \leftarrow \text{La}^-(^3F^e_2)$, is chosen to measure the EA of La because its photodetachment threshold is in the tuning range of our dye laser. See Fig. 2.

To determine the binding energy of peak a as accurately as possible, a series of spectra were obtained near the

TABLE II. The binding energy of bound states of La$^-$, and the energy levels of La$^-$.

State		Binding energy (cm^{-1})		Relative energy (cm^{-1})			
		Theory [18]	This work	Theory [12]	Theory [18]	Experiment[a] [8]	This work
$6s^2 5d^2$	$^3F_2^e$	4436	4496.97(20)	0	0	0	0
	$^3F_3^e$	3799	3819.91(29)	675.5	637	677.0	677.06(35)
	$^3F_4^e$	3081	3102.52(25)	1409.9	1355	1394.2	1394.45(32)
	$^1D_2^e$	2170	2107.63(30)	2646.3	2266		2389.34(36)
	$^3P_0^e$	1113	1405.3(30)	3308.5	3323		3091.7(30)
	$^3P_1^e$	952	1067(60)	3552.1	3484		3430(60)
	$^3P_2^e$	524	452(60)	4070.7	3912		4045(60)
$6s^2 5d6p$	$^1D_2^o$	2549	2700(60)	1757.5	1887		1797 (60)
	$^3F_2^o$	1702		2789.1	2734	2772.0	
	$^3F_3^o$	1299		3138.3	3137	3096.1	
	$^3D_1^o$	1178		3281.9	3258	3221.5	
	$^3D_2^o$	557		3859.4	3880	3795.2	
	$^3F_4^o$	476		4056.2	3960	4002.0	
	$^3P_0^o$	153		4424.8			
	$^3D_3^o$	2549		4430.4	4283	4345.7	

[a]The uncertainty of the measurement by Walter *et al.* [8] is 0.24 cm^{-1}.

threshold of transition La($^2F_{5/2}^e$) ← La$^-$($^3F_2^e$) at the imaging voltage of -350 V. The photon energy $h\nu$ was scanned from 11 525 cm^{-1} to 11 575 cm^{-1} with a step $\sim$10 cm^{-1}, slightly above the threshold. The photoelectrons with the same kinetic energy will form a spherical shell before hitting the phosphor screen and the radius r of the spherical shell is proportional to the velocity of the electrons. Thus, the kinetic energy of photoelectrons $E_k \propto r^2$. Since $h\nu = \text{BE} + \alpha r^2$, the experimental data points are in a straight line if $h\nu$ is plotted versus r^2. Here BE is the binding energy of the observed state, and α is a coefficient to be determined via the energy calibration. As Fig. 3 shows, the intercept of the fitted line is the BE value. Thus, the binding energy of transition La($^2F_{5/2}^e$) ← La$^-$($^3F_2^e$) is determined to be 11 508.88 ± 0.20 cm^{-1}. As a result, the EA value of La is determined to be 4496.97(20) cm^{-1} or 0.557 553(25) eV by subtracting the level energy 7011.909 cm^{-1} of the final neutral La $5d^2 6s\ ^2F_{5/2}^e$ state from 11 508.88 ± 0.20 cm^{-1} [34]. Note that 1 eV = 8065.544 005(50) cm^{-1}, as recommended by 2014 CODATA (Committee on Data for Science and Technology) [36].

According to the known information of La$^-$ and La, peak n is composed of three transitions. The transitions La($^2F_{5/2}^e$) ← La$^-$($^3F_3^e$) (peak n_1) and La($^2F_{7/2}^e$) ← La$^-$($^3F_4^e$) (peak n_2) are not resolved from the transition La($^2F_{3/2}^e$) ← La$^-$($^3F_2^e$) (peak n_3). As the EA value of La is determined, the binding energies of peaks c, n_1, o, r, and u, which are all from state $^3F_3^e$, can be accurately settled, and similarly for peaks b, n_2, p, and t, which are all from state $^3F_4^e$. The binding energies of ($^3F_3^e$) and $^3F_4^e$ are determined to be 3819.91(29) cm^{-1} and 3102.52(25) cm^{-1}. Peak d belongs to the transition La($5d^2 6s\ ^2D_{3/2}^e$) ← La$^-$ ($5d^2 6s^2\ ^1D_2^e$), and the binding energy is 10 553.68(30) cm^{-1}. Thus, the energy

level of La$^-$ ($^1D_2^e$) is determined to be 2107.63(30) cm^{-1}. State ($^1D_2^e$) also contributes to peaks g, v, and x. Note that the spacing between e and j (1812.8 cm^{-1}) is exactly the same as that between $^2P_{1/2}^e$ and $^4P_{1/2}^e$ of lanthanum (1812.807 cm^{-1}). The assignments we obtained are as follows: La($5d^2 6s\ ^2P_{1/2}^e$) ← La$^-$ ($5d^2 6s^2\ ^3P_0^e$) contributes to peak e, and La($5d^2 6s\ ^4P_{1/2}^e$) ← La$^-$ ($5d^2 6s^2\ ^3P_0^e$) for peak j. The binding energy of $^3P_0^e$ is determined to be 1405.3(30) cm^{-1}. According to Pan and Beck's calculations [18], peaks f, i, and k belong to $^3P_{1,2}^e$ states. State $^1D_2^e$ contributes to peak h, which is buried within peaks g and i. The binding energies are estimated as 452(60) cm^{-1} ($^3P_2^e$), 1067(60) cm^{-1} ($^3P_1^e$), and 2700(60) cm^{-1} ($^1D_2^o$) by means of Gaussian multipeak fitting. Peak w is mainly due to the transition La($5d6s^2\ ^2\tilde{D}_{3/2}^e$) ← La$^-$ ($5d6s^2 6p\ ^1D_2^o$). It may include a contribution from the transition La ($5d6s^2\ ^2\tilde{D}_{5/2}^e$) ← La$^-$ ($5d6s^2 6p\ ^3F_2^o$). The lifetime of $^3F_2^o$ is approximately 1 ms according to O'Malley and Beck's calculations in 2010 [37]. Therefore, $^3F_2^o$ can contribute to the spectrum in this regard. Table I lists the assignment in detail. Figure 2 shows the transitions from La$^-$ states which are precisely measured in this work. The states $^3P_{1,2}^e$ are not included for the sake of conciseness. See Table II.

In conclusion, the electron affinity of lanthanum is determined to be 4496.97(20) cm^{-1} or 0.557 553(25) eV. The binding energies of La$^-$ ($5d^2 6s^2$) $^3F_3^e$ and $^3F_4^e$ are measured to be 3819.91(29) cm^{-1} and 3102.52(25) cm^{-1}, respectively. The binding energies of $^1D_2^e$, $^3P_0^e$, and $^1D_2^o$ are also measured: 2107.63(30) cm^{-1} for $^1D_2^e$, 1405.3(30) cm^{-1} for $^3P_0^e$, and 2700(60) cm^{-1} for $^1D_2^o$. The photoelectron spectra also indicate the existence of the states $^3P_1^e$ and $^3P_2^e$, and their binding energies are estimated as 1067(60) cm^{-1} and 452(60) cm^{-1}.

As can be seen, the combination of SEVI and ion trap can provide abundant information of complex anions with bound-bound transitions. This method can be adopted to investigate the complicated electronic structure of other lanthanide and actinide anions.

ACKNOWLEDGMENTS

[1] A. Kellerbauer and J. Walz, New J. Phys. **8**, 45 (2006).

[2] A. Kellerbauer, G. Cerchiari, E. Jordan, and C. W. Walter, Phys. Scr. **90**, 054014 (2015).

[3] R. C. Bilodeau and H. K. Haugen, Phys. Rev. Lett. **85**, 534 (2000).

[4] U. Warring, M. Amoretti, C. Canali, A. Fischer, R. Heyne, J. O. Meier, C. Morhard, and A. Kellerbauer, Phys. Rev. Lett. **102**, 043001 (2009).

[5] U. Warring, C. Canali, A. Fischer, and A. Kellerbauer, J. Phys.: Conf. Ser. **194**, 152022 (2009).

[6] A. Kellerbauer and S. Fritzsche, J. Phys.: Conf. Ser. **388**, 012023 (2012).

[7] L. Pan and D. R. Beck, Phys. Rev. A **82**, 014501 (2010).

[8] C. W. Walter, N. D. Gibson, D. J. Matyas, C. Crocker, K. A. Dungan, B. R. Matola, and J. Rohlen, Phys. Rev. Lett. **113**, 063001 (2014).

[9] C. W. Walter, N. D. Gibson, C. M. Janczak, K. A. Starr, A. P. Snedden, R. L. Field III, and P. Andersson, Phys. Rev. A **76**, 052702 (2007).

[10] C. W. Walter, N. D. Gibson, Y.-G. Li, D. J. Matyas, R. M. Alton, S. E. Lou, R. L. Field III, D. Hanstorp, L. Pan, and D. R. Beck, Phys. Rev. A **84**, 032514 (2011).

[11] E. Jordan, G. Cerchiari, S. Fritzsche, and A. Kellerbauer, Phys. Rev. Lett. **115**, 113001 (2015).

[12] G. Cerchiari, A. Kellerbauer, M. S. Safronova, U. I. Safronova, and P. Yzombard, Phys. Rev. Lett. **120**, 133205 (2018).

[13] A. M. Covington, D. Calabrese, J. S. Thompson, and T. J. Kvale, J. Phys. B: At., Mol. Opt. Phys. **31**, L855 (1998).

[14] S. M. O'Malley and D. R. Beck, Phys. Rev. A **79**, 012511 (2009).

[15] S. H. Vosko, J. B. Lagowski, I. L. Mayer, and J. A. Chevary, Phys. Rev. A **43**, 6389 (1991).

[16] E. Eliav, S. Shmulyian, U. Kaldor, and Y. Ishikawa, J. Chem. Phys. **109**, 3954 (1998).

[17] S. M. O'Malley and D. R. Beck, Phys. Rev. A **60**, 2558 (1999).

[18] L. Pan and D. R. Beck, Phys. Rev. A **93**, 062501 (2016).

[19] A. Osterwalder, M. J. Nee, J. Zhou, and D. M. Neumark, J. Chem. Phys. **121**, 6317 (2004).

[20] D. M. Neumark, J. Phys. Chem. A **112**, 13287 (2008).

[21] I. León, Z. Yang, H.-T. Liu, and L.-S. Wang, Rev. Sci. Instrum. **85**, 083106 (2014).

[22] Z. Luo, X. Chen, J. Li, and C. Ning, Phys. Rev. A **93**, 020501 (2016).

[23] X. Chen, Z. Luo, J. Li, and C. Ning, Sci. Rep. **6**, 24996 (2016).

[24] X. Fu, Z. Luo, X. Chen, J. Li, and C. Ning, J. Chem. Phys. **145**, 164307 (2016).

[25] X. Chen and C. Ning, J. Phys. Chem. Lett. **8**, 2735 (2017).

[26] X.-B. Wang and L.-S. Wang, Rev. Sci. Instrum. **79**, 073108 (2008).

[27] C. Hock, J. B. Kim, M. L. Weichman, T. I. Yacovitch, and D. M. Neumark, J. Chem. Phys. **137**, 244201 (2012).

[28] R. Tang, X. Fu, and C. Ning, J. Chem. Phys. **149**, 134304 (2018).

[29] R. Tang, X. Chen, X. Fu, H. Wang, and C. Ning, Phys. Rev. A **98**, 020501 (2018).

[30] X. Chen and C. Ning, Phys. Rev. A **93**, 052508 (2016).

[31] W. C. Wiley and I. H. McLaren, Rev. Sci. Instrum. **26**, 1150 (1955).

[32] A. T. J. B. Eppink and D. H. Parker, Rev. Sci. Instrum. **68**, 3477 (1997).

[33] B. Dick, Phys. Chem. Chem. Phys. **16**, 570 (2014).

[34] J. E. Sansonetti and W. C. Martin, J. Phys. Chem. Ref. Data **34**, 1559 (2005).

[35] P. C. Engelking and W. C. Lineberger, Phys. Rev. A **19**, 149 (1979).

[36] P. J. Mohr, D. B. Newell, and B. N. Taylor, Rev. Mod. Phys. **88**, 035009 (2016).

[37] S. M. O'Malley and D. R. Beck, Phys. Rev. A **81**, 032503 (2010).